nature plants

PERSPECTIVE

https://doi.org/10.1038/s41477-021-00952-8

Check for updates

Emerging satellite observations for diurnal cycling of ecosystem processes

Jingfeng Xiao[1]✉, Joshua B. Fisher[2], Hirofumi Hashimoto[3,4], Kazuhito Ichii[5] and Nicholas C. Parazoo[2]

Diurnal cycling of plant carbon uptake and water use, and their responses to water and heat stresses, provide direct insight into assessing ecosystem productivity, agricultural production and management practices, carbon and water cycles, and feedbacks to the climate. Temperature, light, atmospheric water demand, soil moisture and leaf water potential vary over the course of the day, leading to diurnal variations in stomatal conductance, photosynthesis and transpiration. Earth observations from polar-orbiting satellites are incapable of studying these diurnal variations. Here, we review the emerging satellite observations that have the potential for studying how plant functioning and ecosystem processes vary over the course of the diurnal cycle. The recently launched ECOsystem Spaceborne Thermal Radiometer Experiment on Space Station (ECOSTRESS) and Orbiting Carbon Observatory-3 (OCO-3) provide land surface temperature, evapotranspiration (ET), gross primary production (GPP) and solar-induced chlorophyll fluorescence data at different times of day. New generation operational geostationary satellites such as Himawari-8 and the GOES-R series can provide continuous, high-frequency data of land surface temperature, solar radiation, GPP and ET. Future satellite missions such as GeoCarb, TEMPO and Sentinel-4 are also planned to have diurnal sampling capability of solar-induced chlorophyll fluorescence. We explore the unprecedented opportunities for characterizing and understanding how GPP, ET and water use efficiency vary over the course of the day in response to temperature and water stresses, and management practices. We also envision that these emerging observations will revolutionize studies of plant functioning and ecosystem processes in the context of climate change and that these observations and findings can inform agricultural and forest management and lead to improvements in Earth system models and climate projections.

Plant scientists and ecologists have been intrigued by the circadian rhythms (or circadian clock) of plants for decades[1,2]. Many compelling science questions have arisen regarding the diurnal (or diel) patterns of plant photosynthesis and transpiration. For example, how do plants use resources throughout the day? How does stomatal conductance change in response to environmental and internal factors (for example, air temperature, light, atmospheric water demand, soil moisture and leaf water potential/storage)? How do plant photosynthesis, transpiration and water use efficiency (WUE) respond to these environmental factors? Addressing these questions is increasingly important in the context of climate change. Increasing water and heat stresses[3,4] can have large impacts on plant functioning and ecosystem processes, particularly during the midday period; plants may exhibit more frequent stomatal closure and midday depression, which can have substantial impacts on plant growth, carbon uptake and plant survival. A better understanding of the responses of plants to water and heat stresses over the course of the day is critical for assessing the impacts of drought and heatwaves on plant production and survival, food security and terrestrial carbon dynamics and for projecting carbon–climate feedbacks.

Elucidating the diurnal cycling of plant water loss by transpiration and carbon gain by photosynthesis is of fundamental importance for understanding how plants interact with ambient and changing environmental conditions. Dissymmetric evolution of stomatal conductance and midday stomatal closure have been shown for different plant species, life stages and ecosystems[5–7]. As a result, photosynthesis can exhibit an afternoon decline and a midday depression[8–10] (Fig. 1), leading to a two-peaked and dissymmetric diurnal pattern[11]. The diurnal variations of stomatal conductance also shape the diurnal pattern of transpiration (Fig. 1). Water stress might result in a larger decrease in evapotranspiration (ET) than in gross primary production (GPP), leading to higher WUE[12]. Water stress may also decrease WUE and lead to less efficient carbon uptake. Diurnal patterns of stomatal conductance, ET and GPP may exhibit large differences among different plant and ecosystem types. A better understanding of the diurnal courses of plant water use and carbon uptake is essential for understanding the relations between water and productivity of natural and managed ecosystems[11], thereby providing insight into the vulnerability and resilience of different ecosystems to drought and/or heat stress[13] and informing management practices (for example, irrigation).

Observations at multiple times of the day are essential for understanding the diurnal cycles of plant water use and carbon uptake. At canopy and ecosystem scales, in situ measurements with portable instruments[14] and the eddy covariance (EC) technique[15,16] have been widely used to examine the diurnal variations of plant functioning and ecosystem processes. In particular, the EC sites provide continuous, sub-hourly measurements of ecosystem carbon and water exchange, meteorological variables and soil moisture[17], which allows scientists to analyse how stomatal conductance, photosynthesis and transpiration vary over the course of the diurnal cycle[15,16].

[1]Earth Systems Research Center, Institute for the Study of Earth, Oceans, and Space, University of New Hampshire, Durham, NH, USA. [2]Jet Propulsion Laboratory, California Institute of Technology, Pasadena, CA, USA. [3]Department of Applied Environmental Science, California State University – Monterey Bay, Seaside, CA, USA. [4]NASA Ames Research Center, Moffett Field, CA, USA. [5]Center for Environmental Remote Sensing, Chiba University, Chiba, Japan. ✉e-mail: j.xiao@unh.edu

Table 1 | Specifications of the instruments/platforms that have diurnal sampling capability in studying plant functioning and ecosystem processes

Instrument	Platform	Launch date	Wavelength	Spatial resolution	Repeat cycle	Spatial extent
ECOSTRESS	ISS	29 June 2018	TIR	70 m	1–5 days	Global (52° N–52° S)
OCO-3	ISS	4 May 2019	Far red, SWIR	2 km	~5 days	Global (52° N–52° S)
AHI	Himawari-8	7 October 2014	Visible, NIR, SWIR, TIR	0.5–2 km	10 min[a]	Eastern Asia and Oceania
ABI	GOES-16	19 November 2016	Visible, NIR, SWIR, TIR	0.5–2 km	10 min[b]	Western Hemisphere
ABI	GOES-17	1 March 2018	Visible, NIR, SWIR, TIR	0.5–2 km	10 min[b]	Western Hemisphere
AGRI	FY-4	10 December 2016	Visible, NIR, SWIR, TIR	0.5–4 km	15 min	Eastern Hemisphere
FCI	MTG	≥2022	Visible, NIR, SWIR, TIR	0.5–2 km	10 min[c]	Europe and Africa
GeoCarb	TBD[d]	≥2022	Far red, SWIR	5–10 km	<1 day	Americas (52° N–52° S)
TEMPO	TBD[d]	≥2022	Red, far red	2.1 × 4.4 km	Hourly	North America
UVN	Sentinel-4	≥2022	Visible, NIR	8 km	Hourly	Europe and North Africa

[a]Himawari-8: 10 min for full disk and 2.5 min for Japan. [b]GOES-16 and GOES-17: 10 min for full disk (with 15 min for full disk before April 2019), 5 min for the conterminous United States and 30 or 60 s at the mesoscale. [c]MTG: 10 min for full disk (Europe and Africa) and 2.5 min for Europe. [d]TBD, to be determined. Both GeoCarb and TEMPO will be deployed on commercial geostationary satellites. NIR, near infrared; SWIR, shortwave infrared.

However, these in situ measurements are spatially sparse and the resulting findings do not necessarily apply elsewhere.

Compared to in situ techniques, satellites can provide direct observations of plants over regions or the globe. Satellites measure plant status, canopy cover, plant productivity, vegetation structure, water stress and other plant or environmental variables. Earth observations from polar-orbiting satellites such as Landsat, Sentinel, Terra, Aqua and Orbiting Carbon Observatory-2 (OCO-2) have been widely used to examine ecosystem processes such as GPP, ET and WUE at regional to global scales[18–21]. However, polar-orbiting satellites typically acquire at best one or two snapshots of a given location during each day or a certain period (for example, 16 days), at the same time of the day or night, and therefore are not designed to study diurnal variations of plant water use and carbon uptake. The carbon and water flux datasets based on these satellite data are available at daily or longer (for example, 8-day) timescales (for example, global GPP and ET products derived from the moderate resolution imaging spectroradiometer (MODIS) aboard Terra and Aqua[18,22]).

Several new and forthcoming Earth-observing satellites have diurnal sampling capabilities. The recently launched ECOsystem Spaceborne Thermal Radiometer Experiment on Space Station (ECOSTRESS) and Orbiting Carbon Observatory-3 (OCO-3), both on board the International Space Station (ISS), provide land surface temperature (LST), ET, GPP and solar-induced chlorophyll fluorescence (SIF) data at different times of the day. New generation geostationary satellites provide continuous observations throughout the day and night. Here, we review these emerging satellite observations (Table 1) and explore the unprecedented opportunities for characterizing and understanding the diurnal cycling of plant functioning and ecosystem processes that have not yet been explored using measurements from space. We also envision how these emerging observations will revolutionize studies of plant functioning and ecosystem processes and how these observations and findings can inform agricultural management and improve Earth system models and climate projections.

ISS: ECOSTRESS

ECOSTRESS was launched to the ISS by the National Aeronautics and Space Administration (NASA) on 29 June 2018 (ref. [23]).

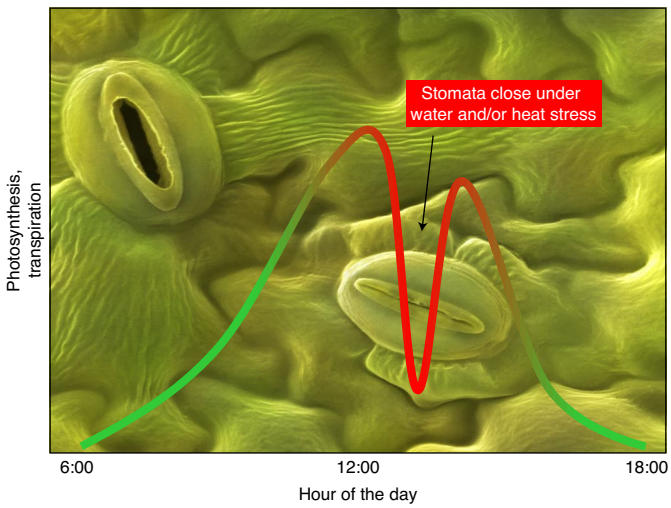

Fig. 1 | Conceptual diagram of plant photosynthesis and transpiration over the course of a day. Both transpiration and photosynthesis may show mid-afternoon depressions due to stomatal closure under water and/or heat stresses. The background image (a coloured scanning electron micrograph) shows open and closed stomata on a lavender leaf (*Lavandula dentata*). Magnification ×2,000 at an image size of 10-cm wide. Stomata are pores on leaves that open and close to regulate the exchange of gases (carbon dioxide, water). Image courtesy of Science Photo Library.

ECOSTRESS measures thermal infrared radiation (TIR) in five bands from 8 to 12.5 μm, plus an additional sixth band at 1.6 μm for geolocation and cloud detection. ECOSTRESS covers the Earth continuously between ~52° N and ~52° S.

ECOSTRESS produces four levels of data products, whereby levels 2–4 are for primary science applications. The pixel size at nadir is 38 × 69 m, which is resampled to 70 × 70-m pixels for higher level data products. The ECOSTRESS science products consist of the following data: LST and emissivity (L2_LSTE)[24,25]; ET including partitioning between canopy transpiration, soil evaporation and interception evaporation (L3_ET_PT-JPL; L3_ET_ALEXI)[23,26];

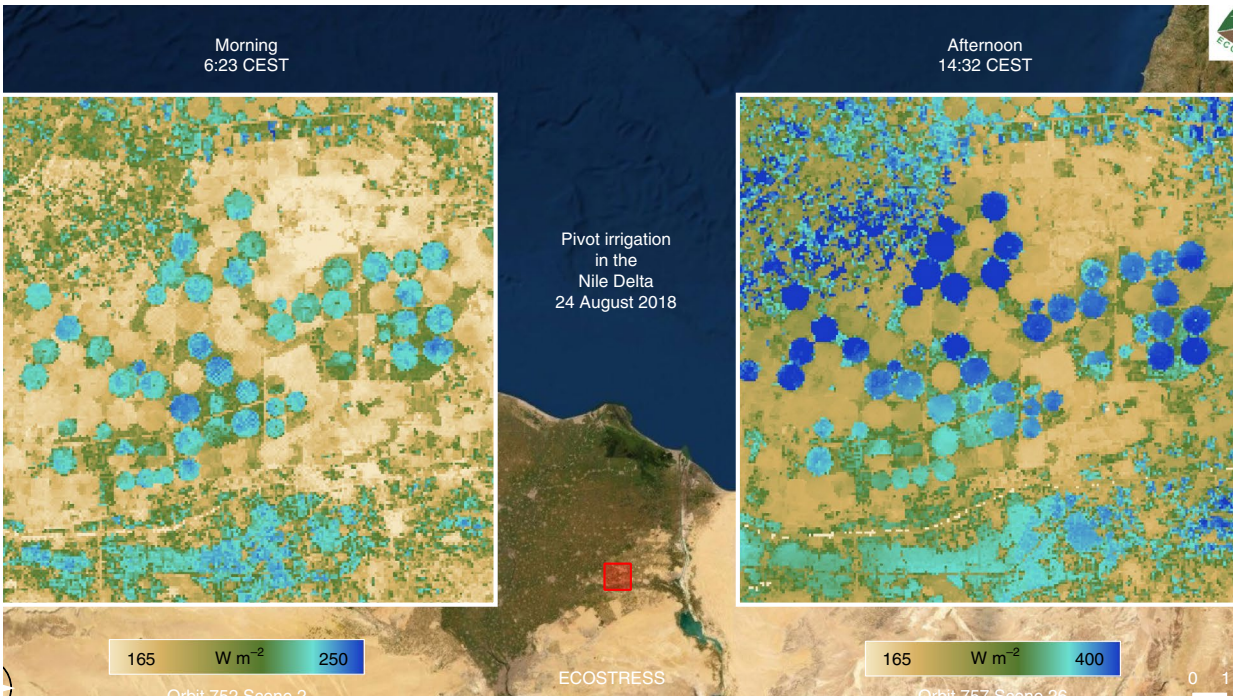

Fig. 2 | ECOSTRESS images from the Nile Delta within the same day. NASA's ECOSTRESS captured changes in ET from agricultural fields of the Nile Delta, Egypt, from the ISS in the morning and afternoon on 24 August 2018. The image on the left is from 6:23 central European summer time (CEST) and the image on the right is from 14:32 CEST. There are larger differences in ET between the agricultural fields in the afternoon than in the morning. Some fields show much more ET while some fields are drying out in the afternoon. The geographical coordinates of the centre of the ECOSTRESS images Orbit 752, Scene 2 (left) and Orbit 757, Scene 26 (right) are 30.54° N and 31.85° E, respectively. The scale bar applies to the background map; the pixel size of the inset maps is 70 m.

the evaporative stress index (ESI)[27]; and WUE (level 4). LST is an instantaneous product, while ET includes both instantaneous and daily estimates. The daily WUE product is calculated from ECOSTRESS daily ET estimates and the MODIS GPP product[18]. Instantaneous WUE can be derived from the instantaneous ET estimates (for example, L3_ET_PT-JPL)[23] and instantaneous GPP estimates[28] based on ECOSTRESS LST data. Field validation showed that the ECOSTRESS LST was in good agreement with in situ measurements with an average root mean square error (RMSE) of 1.07 K, mean absolute error (MAE) of 0.40 K and $R^2 > 0.988$ at all sites[29]. The ECOSTRESS ET product likewise performed well against in situ measurements from 82 EC flux sites ($R^2 = 0.88$, overall bias = 8%, normalized RMSE = 6%)[23].

Flying in the precessing orbit of the ISS, ECOSTRESS collects measurements at different times of the day, thereby sampling the diurnal cycle. The ISS orbit characteristics, in conjunction with the large 384-km ECOSTRESS swath width, enables a return frequency every 1–5 days, depending on the latitude. Higher latitudes, where the ISS orbital direction shifts, are measured multiple times in a single day. ECOSTRESS therefore provides the highest combination of spatial and temporal resolution diurnal sampling of surface properties associated with temperature and water. ECOSTRESS can sample a large portion of the diurnal cycle over a period of weeks.

Diurnally, ECOSTRESS can provide transformative information about plant heat and water stress, and water use. While the diurnal sampling of geostationary satellites such as Himawari-8 and the GOES-R series is more frequent, the coarse spatial resolution (for example, 2 km for TIR bands) produces mixed pixels containing plant species or individuals with different diurnal cycles. The 70-m ECOSTRESS pixels are much closer to the scale of small ecosystem patches and individual agricultural fields. Further spatial downscaling is possible through fusion with other sensors[30]. It is therefore possible to detect from space, for example, individual fields drying out in the afternoon (Fig. 2)—this has never been possible in the history of remote sensing before ECOSTRESS. This type of information can be returned to farmers and water managers who may not know that individual fields could use more water. Similarly, it may be possible to see parts of a forest drying out before other parts, such as forest edges—again, information that can be critically useful for forest and fire managers. While diurnal water stress is certainly not a new phenomenon, until ECOSTRESS, we did not know where and when this was occurring globally. This type of science application requires that satellite instruments offer observations with <100-m pixel size, <10% relative uncertainty and <weekly repeat cycle.

From a plant ecophysiological perspective, we are interested in stomatal closure induced by water, temperature and vapour pressure deficit (VPD)[31]. We know from local in situ measurements that some plants close stomata in response to these stressors[32]. However, not all plants behave the same even within the same area or species, for example, due to variations in rooting depth, soil moisture and/or water table, and/or due to differences in species, age and/or disturbance history[33]. Although we know that these differences exist from local measurements, we do not know where these responses are occurring globally. This is where ECOSTRESS can advance plant ecophysiological science.

The suite of ECOSTRESS products can be used synergistically to understand diurnal cycles of plant water and temperature responses. From the state-of-the-art number of TIR spectral bands and retrieval approach[34], the LST data can map with great precision both the instantaneous heat of the plant surface and the duration that the heat might extend into the day and night[25]. How that heat dissipates in time and space is related both to surface physical properties and water use (in the absence of exogenous factors). In turn, the ET data reveal how much water is used throughout the day and

how that water use deviates from expectations due to atmospheric demand alone[35]. The canopy transpiration product can be used to isolate the plant contribution to total ET[36]. The ESI product is useful for diagnosing attribution to ET responses, as well as the lead up before ET responses and drought impacts[37]. GPP estimates based on ECOSTRESS LST data can reveal how plant photosynthesis varies throughout the day in response to variations in environmental and physiological factors and management practices (for example, irrigation)[28]. Finally, the WUE product can link water and temperature responses to carbon cycle processes and to synergistic measurements from other sensors, such as SIF from OCO-3, another ISS instrument[38].

ISS: OCO-3

The OCO-3 was deployed to the ISS in May 2019 and has been collecting joint measurements of atmospheric CO_2 and plant SIF since August 2019 (ref. [39]). Unlike its polar-orbiting predecessor (OCO-2)[40], OCO-3 samples reflected sunlight in the tropics and subtropics across the full range of daylight hours (dawn to dusk), with dense observations at northern and southern mid-latitudes (±52°), like ECOSTRESS, due to the low-inclination ISS orbit. OCO-3 also has a snapshot area mode (SAM), and this technical innovation enabled localized mapping of SIF for the first time. By continuing the concurrent SIF observations of OCO-2 in time, expanding OCO-2 measurements in space and focusing on ecosystem and urban hotspots, OCO-3 provides scientists a unique vantage of the processes that influence the global carbon cycle and plant behaviour, thus increasing our understanding of how global climate patterns affect the terrestrial carbon cycle.

Plant fluorescence has been studied in laboratories and the field for several decades, with a focus on plant-level photosynthesis[41]. When plants absorb solar energy for growth, they re-emit a small amount (~2%) of sunlight back to space. Although SIF exhibits a complex and varying relationship with photosynthesis at various scales (for example, leaf, canopy and ecosystem)[42,43], ecosystem-resolving spaceborne sensors such as GOME-2, GOSAT, OCO-2 and TROPOMI found a simple linear relationship between fluorescence and rates of ecosystem-scale photosynthesis observed at towers, nearly independent of vegetation type[21,44,45]. This allows scientists to use empirical relationships to estimate global rates of photosynthesis[46], its change over time and space, and to study its climate sensitivity (for example, the photosynthesis of tropical continents responded in different ways to warming and drying during the 2015–2016 El Niño)[47]. The intercomparison of SIF between OCO-3 and its predecessor (OCO-2) showed that OCO-3 SIF is of comparable quality to OCO-2 SIF[39], which shows strong seasonal agreement with tower and airborne SIF measurements at a subalpine evergreen forest[48], and correlates well with tower-based GPP across multiple biomes (with R^2 values ranging from 0.73 to 0.81)[21,44].

While OCO-2 offers the high spectral resolution needed to capture the downregulation of photosynthesis under increasing water limitation[49], it misses the full dynamic range of water stress responses due to fixed afternoon sampling during peak stress (~13:30 local time). Moreover, attempts to combine afternoon measurements from one polar-orbiting satellite (TROPOMI) with morning measurements from another satellite (GOME-2) revealed systematic orbital geometry-dependent variations that masked physiologically driven diurnal changes. A recent analysis of the FLUXNET2015 EC database showed that photosynthesis in most plant types typically peaks in late morning before peak potential shortwave incoming radiation, when water stress is low and boundary layer CO_2 is high, then decreases in the afternoon with lower light-use efficiency[50]. ET, meanwhile, typically peaks in the afternoon with VPD, creating a diurnal hysteresis between ecosystem fluxes that is typically and critically unresolved by polar-orbiting satellites.

OCO-3 provides the diurnal sampling and spatial resolution needed to advance our understanding of photosynthesis, especially under heat and water stress. OCO-3 passes over any given location (at nadir) ~20-min earlier each time, eventually sampling all sunlit hours[39]. Each time the instrument passes over, it collects SIF snapshots (1–2-km footprints) capable of resolving photosynthetic CO_2 uptake at the ecosystem. These measurements provide scientists with a new level of detail on the interaction between ecosystem-scale photosynthetic processes and drought responses.

OCO-3 target and SAM observations offer versatile alternatives to the narrow (~10 km) nadir and glint swaths for the collection of dense, cloud-free, spatially resolved datasets at selected ecosystem hotspots and validation targets. OCO-3 scans a repeated swath over ~20 × 20-km areas in the target mode and adjacent swaths over ~80 × 80-km areas in the SAM mode. Target data are used primarily for CO_2 calibration and validation but offer high-precision, diurnally and seasonally resolved SIF across a small subset of locations around the world. SAM data provide SIF across a wide variety of urban, volcanic, agricultural and naturally vegetated locations to study biological exchange in managed and unmanaged landscapes. SAM locations can also be reprogrammed for the near-real-time study of climate extremes (for example, drought, flooding or fires), weather extremes (for example, hurricane or derecho) and changes in management (for example, irrigation and water-use restrictions).

The OCO-3 observations overlap in space and time with ECOSTRESS due to the shared ISS platform, although ECOSTRESS covers even more area due to its larger swath. A large percentage of SAM collection is coincident with ECOSTRESS priority EC validation sites. While the nature of the precessing ISS orbit can cause irregular spatial sampling, the extended spatial coverage enables more focused analyses of cloud-free subregions with overlapping coverage in time. For example, a series of SAMs collected at the Santa Rita Experimental Range in Arizona, United States, demonstrated the impact of sporadic sampling and clouds on spatial maps (Fig. 3), but careful downsampling and quality control produced an aggregated sounding and diurnal signature that resembles observations from ground-based measurements[48,51,52]. OCO-3, in combination with ECOSTRESS, provides cutting-edge insight into ecosystem processes of SIF and ET and ultimately can be combined as WUE, with high-resolution sampling throughout the day. While certainly an advance over predecessor measurements, both instruments still do not continuously observe the diurnal cycle; therefore, synergy with geostationary instruments can help close this loop.

New generation geostationary satellites

Although ECOSTRESS and OCO-3 have diurnal sampling capabilities, these samples are not continuous throughout the day for a given location. By contrast, geostationary satellites carry optical sensors with high-frequency observation capability (10–15 min in full scan mode). With such high temporal frequency and spectral features, these satellites are expected to improve diurnal monitoring of ecosystem dynamics[53]. Following Himawari-8 (launched in 2014) with the advanced Himawari imager (AHI)[54], the subsequent geostationary satellites carry the same type of optical sensors: advanced baseline imager (ABI) on the geostationary operational environmental satellite-R series (GOES-R) (GOES-16 launched in 2016 and GOES-17 launched in 2018)[55] and advanced meteorological imager (AMI) on GEO-KOMPSAT-2A (GK-2A) (launched in 2018)[56]. These instruments collect high-frequency observations of radiance in both solar reflective and TIR wavelengths. New sensors with similar features are also aboard China's and Europe's new generation geostationary satellites: advanced geostationary radiation imager (AGRI) on Fengyun-4 (FY-4) series (FY-4A was launched in 2016)[57] and flexible combined imager (FCI) on Meteosat third generation (MTG) series[58]. The combination of observations from these satellites (Table 1) can presumably cover the entire globe and enable the

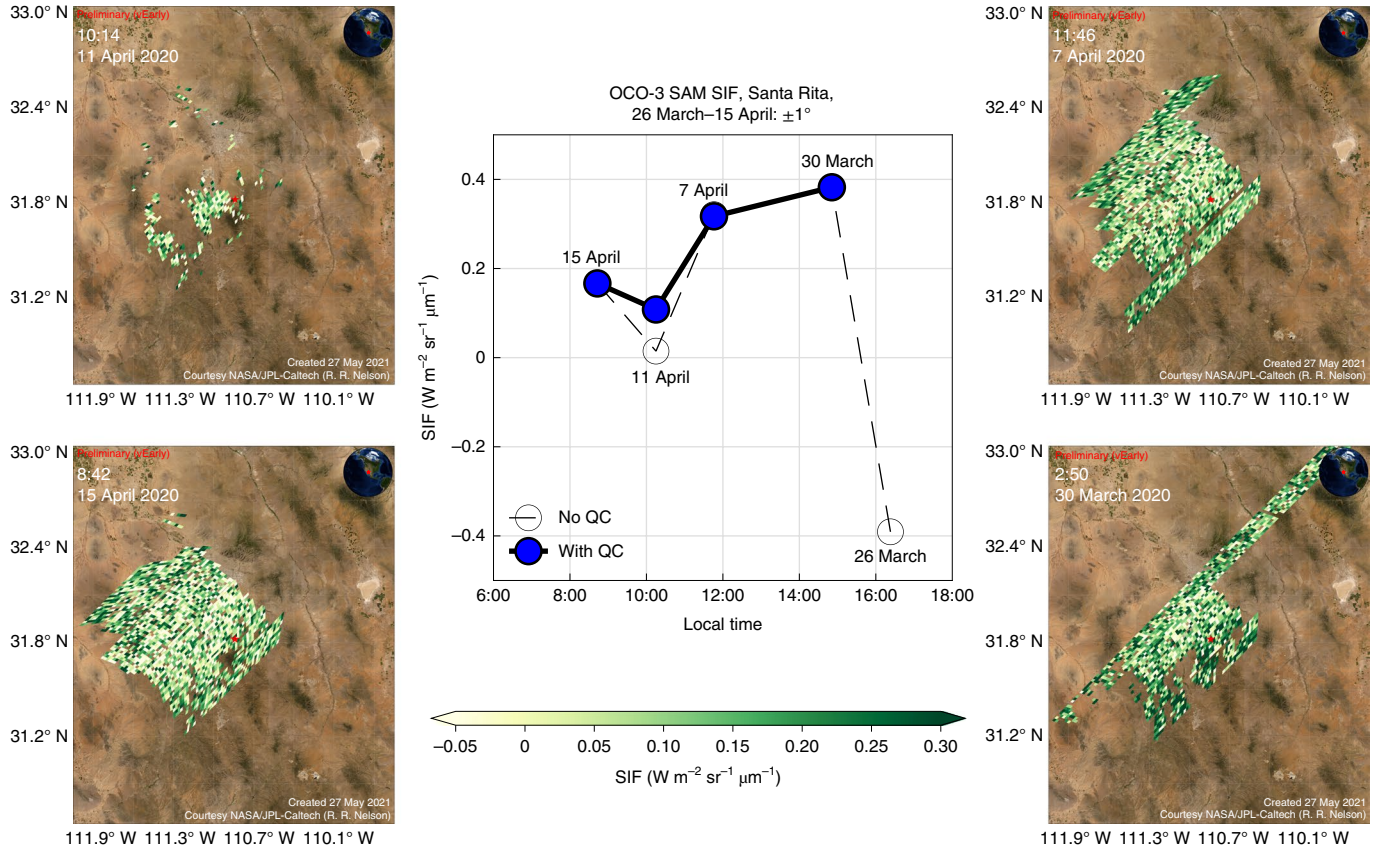

Fig. 3 | SIF at different times of the day as measured by the OCO-3 in SAM mode. The SIF data, a proxy of plant photosynthesis, were acquired surrounding the Santa Rita Experimental Range, Arizona. The four maps show the spatial patterns of SIF at the landscape scale for different times of day in March and April 2020. The centre plot illustrates the diurnal variations of SIF spatially averaged within the 0.1 × 0.1° area surrounding the Santa Rita Experimental Range research site; the blue and white symbols indicate the uses of data with quality control (QC; solar zenith angle of <70°, view zenith angle of <40° and cloud fraction of <0.1) and no QC, respectively.

monitoring of any place on the Earth with a high frequency. For example, the Copernicus Global Land Service (https://land.copernicus.eu) now provides LST data for a large portion of the Earth's land surface (Supplementary Fig. 1). GeoNEX, a collaborative effort among NASA and agencies/organizations in other countries such as Japan and Korea, is generating Earth-monitoring products from the new generation geostationary satellites[59].

TIR images with improved spectral, spatial and temporal resolution can lead to more accurate and more frequent LST retrievals compared with previous geostationary measurements[60]. For example, the GOES-16 LST had good agreement with in situ measurements (overall bias of −0.84 K)[61], and the Himawari-8 LST was also able to estimate LST fairly well (RMSE ≤0.9 K)[60]. These observations can be used to understand how environmental stresses influence ET and GPP throughout the day. Furthermore, incoming solar radiation, which is a primary driver of photosynthesis, is available from geostationary satellites[62]. These geostationary satellite data can lead to high-frequency estimates of ecosystem processes throughout the day.

For example, we mapped hourly GPP values over Australia at the hourly time step using the Himawari-8 AHI data and a light-use efficiency model[63] (Fig. 4). The meteorological input data, including solar radiation, air temperature and VPD, were estimated from AHI visible and thermal bands and ground meteorological data using machine-learning techniques. The MODIS fraction of absorbed photosynthetically active radiation product[64] was corrected using the normalized difference vegetation index time series derived from AHI. The comparison of the satellite-derived GPP to tower GPP from four EC flux sites showed consistent magnitude and diurnal patterns of hourly GPP (Supplementary Figs. 2 and 3). The resulting GPP product estimates the gross carbon uptake of terrestrial ecosystems in Australia for each hour of the day. Fig. 4 illustrates how GPP varied over space for every 2 h of the day and how GPP changed over the course of the day for each location across the Northern Territory.

Future missions

Several future missions also have planned diurnal sampling capabilities for ecosystem science (Table 1). The geostationary carbon cycle observatory (GeoCarb), a NASA mission with a currently planned launch as early as 2022, will measure CO_2, methane, carbon monoxide and SIF[65]. GeoCarb will be hosted in geostationary orbit at 85° W and will measure SIF over North and South America at 5–10-km resolution. GeoCarb will use O_2 and CO_2 channels that are similar to those used for the OCO-2 and will use the OCO-2 algorithm for SIF retrieval. Whereas other SIF sensors have narrow swaths, GeoCarb can measure every pixel in a scan block in a few hours. In the block scan mode, GeoCarb can measure SIF at the same place only once or twice a day, like a sampler as opposed to a continuous recorder, depending on the scan blocks. However, the flexible scan strategy of GeoCarb enables the measurement of SIF at the target area multiple times per day when using the intensive scan mode. NASA will also install the tropospheric emissions: monitoring of pollution (TEMPO)[66] instrument on a commercial geostationary

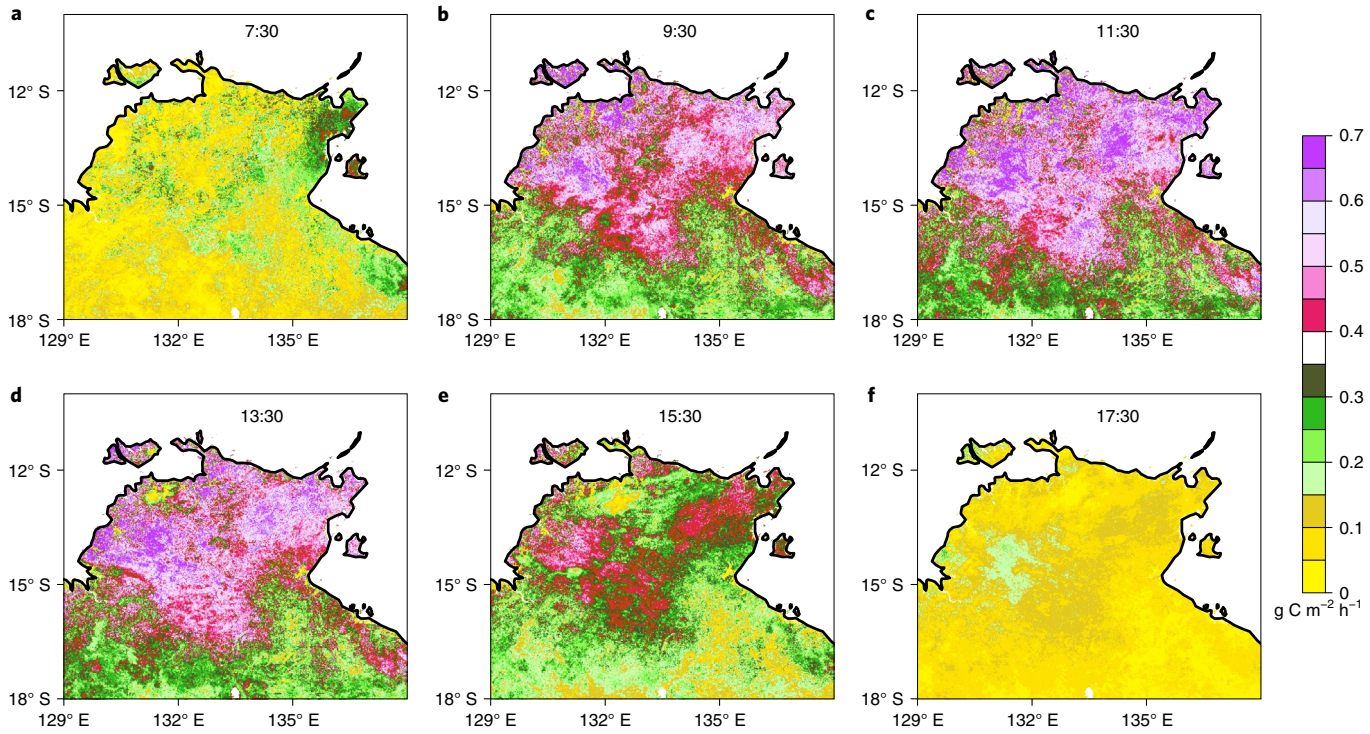

Fig. 4 | Diurnal variations in plant photosynthesis derived from geostationary satellite data and a light-use efficiency model. a–f, The Himawari-8 AHI captured hourly variations in plant photosynthesis (that is, GPP) over the Northern Territory, Australia, every 2 h from 7:30 to 17:30 (Australian central time) on 1 February 2018. The figure indicates that geostationary satellite data can be used to examine diurnal variations of ecosystem functioning.

satellite in as early as 2022. TEMPO is mainly designed for monitoring air pollution, but has the capability of measuring SIF in both red and far-red wavelengths. TEMPO will cover North America with hourly frequency. However, the spectral resolution of TEMPO is coarse (0.6 nm); therefore, any SIF retrievals should be considered experimental. The European Space Agency also has a planned similar geostationary mission, Sentinel-4, focusing on monitoring air pollution[67]. Sentinel-4 will cover Europe hourly with the ultraviolet visible near-infrared (UVN) imaging spectrometer at 8-km resolution. Compared to OCO-3, which collects measurements globally between ~52° N and ~52° S, these future missions (that is, GeoCarb, TEMPO and Sentinel-4) will provide SIF observations at the continental scale. These SIF observations, when combined, will be valuable for capturing the diurnal variations of photosynthesis. With high frequency, TEMPO and Sentinel-4 missions can lead to increased cloud-free SIF retrievals. Although the combined use of the SIF data from these sensors can cover larger spatial domains, these SIF data will be based on different wavelengths and will have different quality. In addition, SIF measured by geostationary satellite sensors can have a large range in the view zenith angle; therefore, the effects of view angle on SIF should be considered in analyses.

A small satellite (SmallSat) constellation can also potentially monitor the diurnal variations of vegetation status. SmallSat constellations have been well developed by commercial companies[68], and some of them can be used to monitor diurnal variations of ecosystem processes. For instance, Planet operates more than 100 SmallSats. Some of their satellite constellations, on an orbit similar to that of the ISS, can acquire observations for different times of day for each location with multiple optical bands and 0.5–3.7-m resolution[69]. For example, Planet's SmallSats can be used to retrieve ET using the same algorithm as ECOSTRESS as well as a fused Planet–ECOSTRESS retrieval[30]. Although these commercial satellite data are not free of charge, they provide increasing opportunities for studying ecosystem processes. A planned NASA SmallSats mission, time-resolved observation of precipitation structure and storm intensity with a constellation of SmallSats (TROPICS)[70], will consist of 12 CubeSats and provide high-frequency (21 min) observations of temperature profile, humidity profile and precipitation. TROPICS is not designed to monitor ecosystems, but can contribute to the diurnal cycling analyses of ecosystem processes given the high frequency of the observations.

Studies of diurnal cycling of ecosystem functioning will also be able to greatly benefit from new ideas for missions that can integrate the advantages of these existing and forthcoming platforms. Ideally, such potential missions will be based on geostationary platforms but will offer observations of LST with fine resolutions equivalent to that of ECOSTRESS and observations of SIF with spatial resolutions equivalent to that of OCO-3. While missions such as ECOSTRESS and OCO-3 are likely to continue well past their prime missions (for example, ECOSTRESS is already an extended mission, having recently been approved for continuity in the NASA Senior Review), the shared platform of the ISS will perpetually introduce complex international negotiations over shared resources. Therefore, new missions that can extend these types of measurements are highly warranted. Still, the science and engineering communities must overcome current engineering limitations, costs and trade-offs associated with the high-altitude geostationary orbits and the demand for high spatial, temporal and spectral resolution.

Synergies

Emerging satellite diurnal observations can be synergistically used to gain new insights into plant functioning and ecosystem processes. ECOSTRESS and OCO-3, which normally would be unlikely pairs on the same mission platform, are now together afforded by the ISS. The combination of the data from these two instruments can allow us to examine plant transpiration and photosynthesis simultaneously and the coupling of these two processes for various types of ecosystems across the globe. Notably,

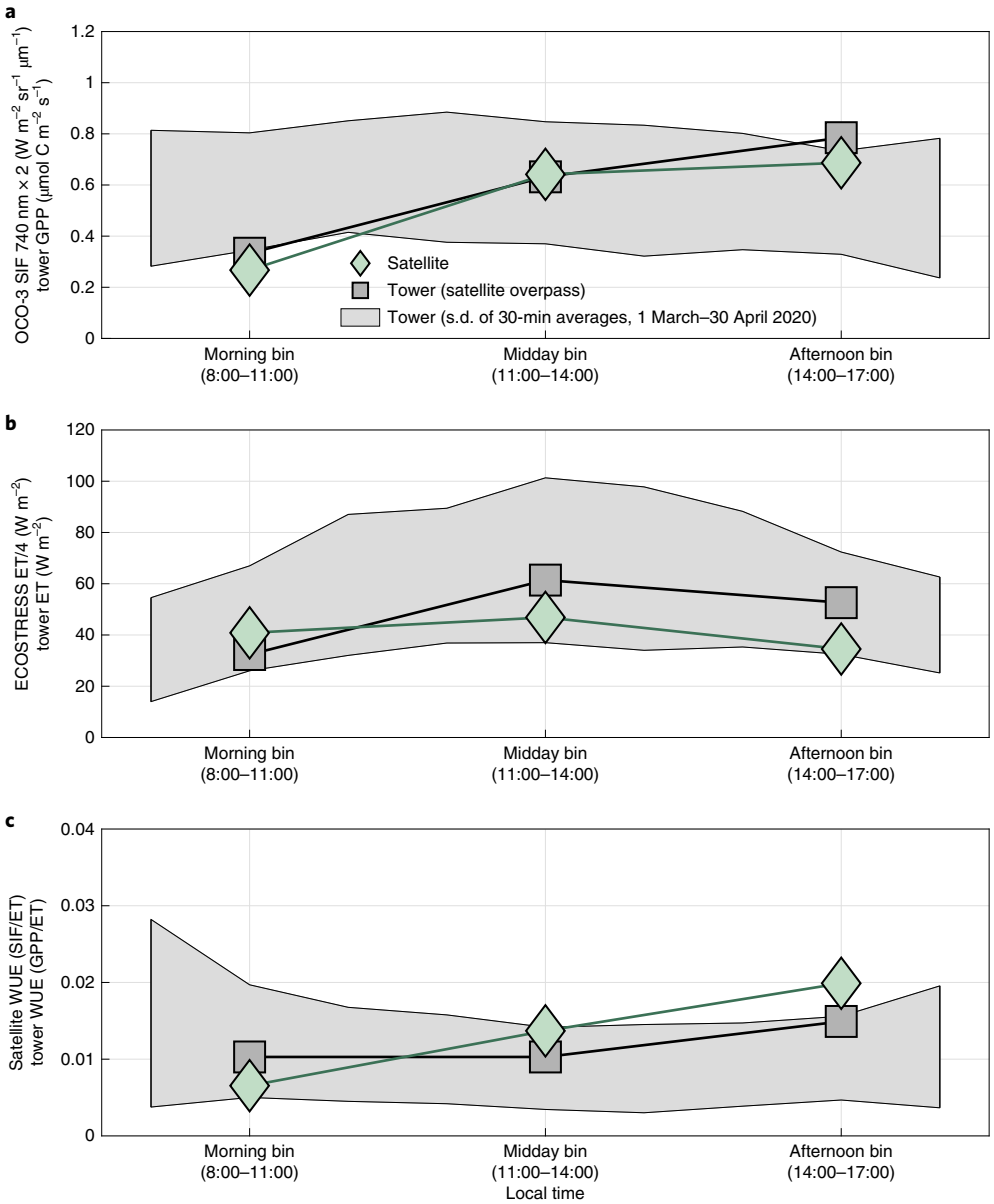

Fig. 5 | The synergy between ECOSTRESS and OCO-3 data enables diurnal monitoring of WUE of terrestrial ecosystems. a–c, The ECOSTRESS ET, OCO-3 SIF (740 nm) and tower data at the Santa Rita Experimental Range, Arizona (31.82° E, 110.87° W), illustrate how OCO-3 SIF and tower GPP (**a**), ECOSTRESS ET and tower ET **(b)** and satellite and tower WUE **(c)** vary over a portion of the diurnal cycle spanning morning, midday and afternoon hours. Here, satellite-derived WUE ($W\,m^{-2}\,sr^{-1}\,\mu m^{-1}/W\,m^{-2}$) is defined as the ratio of SIF to ET, while tower-based WUE ($\mu mol\,C\,m^{-2}\,s^{-1}/W\,m^{-2}$) is defined as the ratio of GPP to ET. The data were acquired between 1 March and 30 April 2020. The SIF and ET data were grouped into 3-h bins (8:00–11:00, 11:00–14:00 and 14:00–17:00, local time) for the calculation of WUE.

the synergistic combination of OCO-3 SIF and ECOSTRESS ET can also provide a measure of WUE. Therefore, the synergistic use of ECOSTRESS and OCO-3 data can allow us to examine how plants use water and absorb carbon over the course of the diurnal cycle, and when, why and how carbon and water uptake couple and decouple from one another. Figure 5 illustrates the variations in SIF, GPP, ET and WUE over a portion of the diurnal cycle at the Santa Rita Experimental Range, Arizona, based on ECOSTRESS and OCO-3 data acquired between 26 March and 15 April 2020. Although the coincident diurnal measurements of ECOSTRESS and OCO-3 can directly provide diurnal measures of WUE that probably have lower uncertainty, it should be noted that OCO-3 does not offer wall-to-wall SIF coverage and has coarse resolution, and that the combination of instantaneous ECOSTRESS ET estimates[23] with instantaneous ECOSTRESS GPP estimates[28] can lead to wall-to-wall and finer-resolution WUE estimates.

Observations from ECOSTRESS and OCO-3 can also be synergistically used with data from geostationary satellites. ECOSTRESS and OCO-3 provide broader global-scale spatial coverage than any geostationary satellite; therefore, consistent studies of this scale are more straightforward from a single ISS platform than piecing together multiple satellites from different geostationary platforms. Despite the diurnal sampling capability, ECOSTRESS and OCO-3 provide only one or few (or no) observations for each location during a given day; therefore, capturing a large portion of the diurnal cycle will require ISS overpasses over a relatively long period

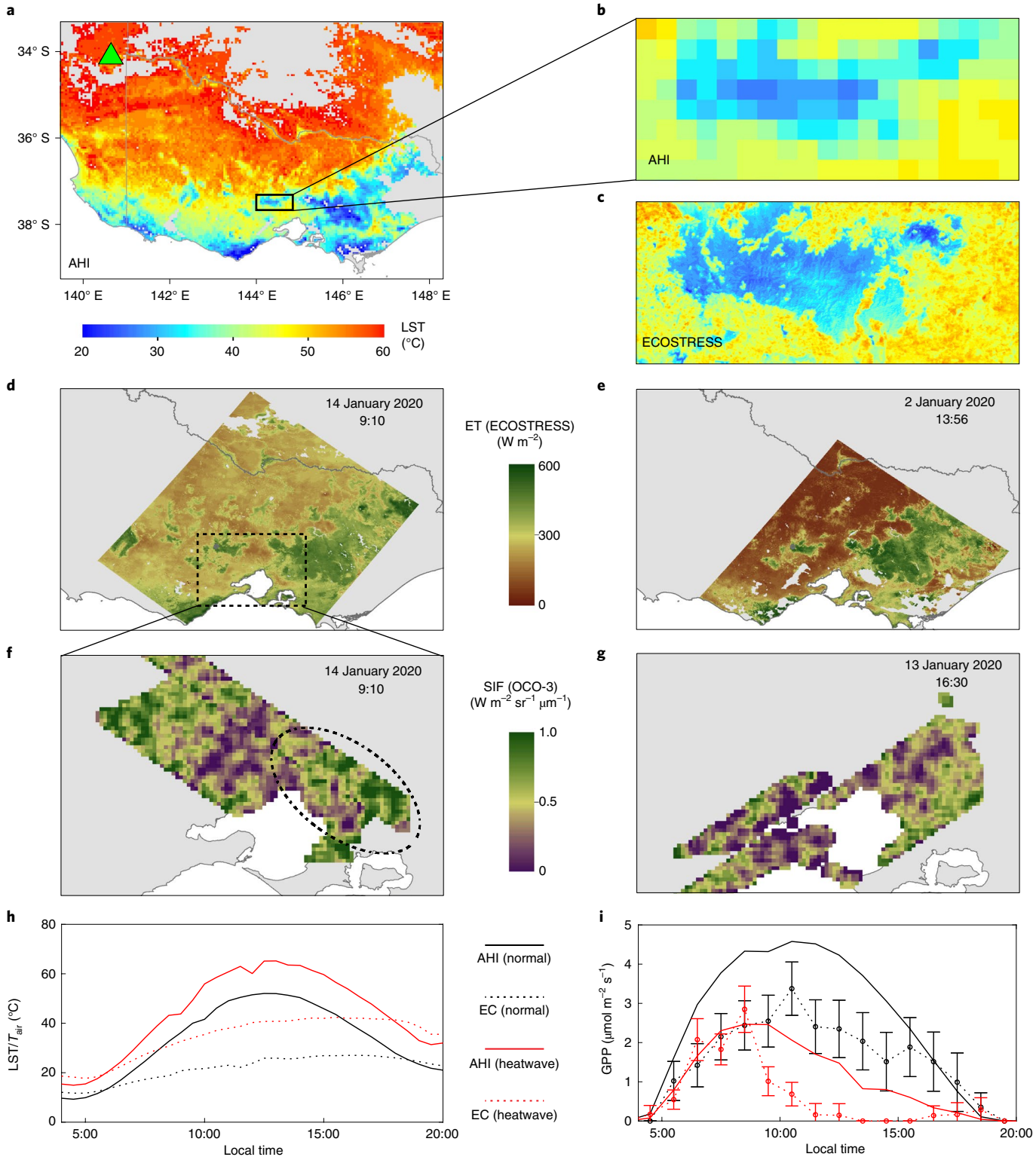

Fig. 6 | Synergistic use of observations from a geostationary satellite and two ISS instruments for studying diurnal cycling of ecosystem processes. Two heatwaves in Australia (2018 and 2020) were studied. **a**, Himawari-8 AHI LST at 13:30 on 2 January 2020 for southern Australia and the location of the EC flux site (Calperum Chowilla, location indicated by the green triangle). **b**,**c**, The coarse-resolution AHI LST (**b**) and fine-resolution (**c**) ECOSTRESS LST (13:55 on 2 January 2020) for the small area highlighted by the rectangle in **a**. **d**,**e**, Instantaneous ECOSTRESS ET for different times of the day. **f**,**g**, Instantaneous OCO-3 SIF for different times of the day. The highlighted area with an ellipse exhibits relatively high SIF in the early morning but low values in the late afternoon. **h**, Diurnal variations in LST (AHI) and air temperature (T_{air}) for a normal day (22 December 2018) and a heatwave day (26 December 2018) at the EC site. **i**, Diurnal variations in AHI-based GPP estimates and flux tower GPP for both the normal and heatwave days at the EC site; the error bars indicate the uncertainty associated with flux partitioning. All times are local time.

(for example, weeks). Over such a period of time, the variations in instantaneous LST, ET or SIF are caused by not only diurnal variations in meteorological conditions and water/heat stress but also the day-to-day variations in these factors, vegetation structure (or leaf area index) and/or phenology, which can complicate diurnal cycle analyses to a certain extent. Compared to these instruments, new generation geostationary satellites such as Himawari-8 and the GOES-R series provide continuous observations throughout the day. However, ECOSTRESS has a much finer spatial resolution (70 m) than geostationary satellites (for example, 2 km) and allows the identification of ecosystem patches or individual fields of croplands. The observations from these instruments can be synergistically used to study the diurnal variations of ecosystem processes by taking advantage of the temporally continuous nature of the geostationary satellite observations throughout the day and the much finer spatial resolution of the ECOSTRESS data. With data fusion techniques[71], for example, the observations from these satellites/instruments can also potentially be merged to generate new data that are temporally continuous over the course of the day and have fine spatial resolution.

As an illustration, the combined use of the data based on Himawari-8 AHI, ECOSTRESS and OCO-3 allowed us to examine how plant photosynthesis and transpiration changed over the course of the day in response to heat and/or water stress in southern Australia (2018–2019 and 2019–2020) (Fig. 6). The LST data of Himawari-8 AHI cover the entire region (Fig. 6a) and beyond (Australia and eastern Asia). Compared to Himawari-8 AHI, ECOSTRESS acquired a limited number of observations but offered much more spatial detail (Fig. 6b,c). The instantaneous ET estimates based on ECOSTRESS showed that with heat and water stress, grasslands and croplands (light green and brown areas) exhibited much lower ET in the early afternoon than in the early morning (~9:00), whereas forests (bright-green areas), with much higher elevation and deeper roots, had only slightly higher ET in the early afternoon than in the early morning (Fig. 6d,e). Meanwhile, SIF data from OCO-3 revealed differences in photosynthesis among different times of day and indicated that plants (in the area highlighted by the ellipse) had high photosynthesis in the early morning but had low values around 16:30 (Fig. 6f,g). Compared to the ISS instruments, AHI provides high-frequency observations throughout the day and makes it feasible to examine the full diurnal cycles of LST and GPP (Fig. 6h,i). The LST on the heatwave day exceeded 40 °C from ~9:00 to ~18:00 and 60 °C from ~11:00 to ~16:00, and the stomatal closure due to water and heat stresses led to a substantial decline in transpiration and a large increase in canopy temperature (Fig. 6h). The hourly GPP based on AHI and the in situ GPP based on an EC flux site showed large and rapid declines from late morning to the middle of the afternoon with the onset of heat stress over a 4-day period (22–26 December 2018) and exhibited midday depression (Fig. 6i). The AHI GPP captured the diurnal variations in EC GPP for both normal ($R^2 = 0.93$, $P < 0.0001$) and heatwave ($R^2 = 0.60$, $P < 0.0001$) days. This example indicates that we can explore diurnal cycling of ecosystem processes from space using these unique datasets together.

The observations from ECOSTRESS, OCO-3 and new generation geostationary satellites also have anticipated synergies with those from the forthcoming missions. For example, the SIF data from OCO-3 and GeoCarb can be directly integrated for ecosystem studies over the Americas. Taken together, the observations from these two missions will cover a 13–18-year period starting from 2019, allowing continued exploration of diurnal photosynthesis at interannual and decadal scales. For example, this will make it possible to examine how the increasing atmospheric CO_2 concentrations influence stomatal behaviour and plant photosynthesis. The SIF data from OCO-3, GeoCarb and TEMPO can also be synergistically used by taking advantage of the higher-quality data from OCO-3 and GeoCarb and high-frequency measurements from TEMPO.

Besides the synergies among these emerging observations, these data can be used in combination with data from polar-orbiting satellites (for example, Terra, Aqua, Suomi NPP, JPSS, Landsat, Sentinel, OCO-2 and SmallSats) and in situ measurements. Polar-orbiting satellites provide observations of vegetation for the globe over multiple decades. These data products such as vegetation indices and leaf area index can be used to provide additional essential variables or extend spatial or temporal domains for the diurnal cycle analyses based on the emerging observations with diurnal sampling capability. Moreover, because of the polar orbit, Terra and Aqua have sizeable swath overlap at the high latitudes (for example, the Arctic), and the resulting larger number of observations can potentially be used for diurnal cycling studies.

In situ measurements have been traditionally used to study diurnal cycling of ecological and physiological processes. For example, previous studies used leaf-level measurements to understand the responses of stomata, leaf photosynthesis and transpiration to soil water content, leaf water potential and VPD[5,32] and midday depression of photosynthesis[72]. Ground measurement networks for water, carbon and energy fluxes such as FLUXNET[17] and the National Ecological Observatory Network (NEON)[73] provide continuous half-hourly measurements and ancillary ecological and environmental data. These data have been used to examine the diurnal cycling of ecological and physiological processes, such as the influence of heat and water stresses on canopy conductance, ET, GPP and WUE[16], physiological responses of carbon–water coupling to hydraulic and non-stomatal limitations[15], and hysteresis patterns of ET and GPP[50]. The emerging satellite observations for diurnal cycling of ecosystem processes make it feasible to explore these ecophysiological processes and phenomena at expanded spatial scales (for example, ecosystems, regions, the globe) from space. Ecophysiological understanding based on in situ measurements will inform and facilitate the exploration of plant water stress and carbon uptake at the regional to global scales using the measurements from space. Data from ECOSTRESS, OCO-3 and the new generation geostationary satellites can be directly linked with half-hourly or hourly flux data to quantify GPP, ET and/or WUE over regions or the globe for different times of day.

Conclusions

Diurnal cycling of plant functioning and ecosystem processes is of fundamental scientific importance for understanding plant water use and carbon uptake in response to water and heat stress, changing climate, rising atmospheric CO_2 and management practices. We envision that the emerging satellite observations reviewed in this Perspective will trigger numerous research efforts aimed at understanding how plant carbon uptake and water use vary over the course of the diurnal cycle from ecosystem to the globe. Data from ECOSTRESS, OCO-3, new generation geostationary satellites (for example, Himawari-8, GOES-R series) and future missions with diurnal sampling capability (for example, GeoCarb, TEMPO and Sentinel-4) are anticipated to be used both individually and synergistically. These observations will probably revolutionize studies of ecosystem processes and carbon and water cycling to a certain extent. The resulting analyses can help us better understand the resilience and vulnerability of different ecosystem types to drought and heatwaves. For croplands, these data can reveal how plant water use varies throughout the day and how irrigation influences ET, water stress and photosynthesis, and the findings can inform agricultural management (for example, irrigation strategies). The instantaneous estimates of ecosystem processes at regional to global scales over the course of the diurnal cycle will also be useful for calibrating and validating Earth system models. A better understanding of how ecosystem processes respond to water and heat stress, changing climate and rising atmospheric CO_2 with the emerging satellite observations can guide improvements to Earth

system models and projections of carbon and water dynamics and carbon–climate feedbacks.

Reporting Summary. Further information on research design is available in the Nature Research Reporting Summary linked to this article.

Data availability

The data that support the findings of this study are available from https://earthdata.nasa.gov (ECOSTRESS), https://lpdaacsvc.cr.usgs.gov/appeears/ (ECOSTRESS), https://ocov3.jpl.nasa.gov/science/oco-3-data-center/ (OCO-3), http://data.ozflux.org.au (flux tower data), https://data.nas.nasa.gov/geonex/ (Himawari-8), ftp://hmwr829gr.cr.chiba-u.ac.jp/gridded/FD/V20151105/ (Himawari-8) and https://land.copernicus.eu/global/products/ (global geostationary satellite LST data).

Received: 3 November 2020; Accepted: 25 May 2021;
Published online: 1 July 2021

References

1. Hennessey, T. L., Freeden, A. L. & Field, C. B. Environmental effects on circadian rhythms in photosynthesis and stomatal opening. *Planta* **189**, 369–376 (1993).
2. Steed, G., Ramirez, D. C., Hannah, M. A. & Webb, A. A. R. Chronoculture, harnessing the circadian clock to improve crop yield and sustainability. *Science* **372**, eabc9141 (2021).
3. Zhao, T. B. & Dai, A. G. The magnitude and causes of global drought changes in the twenty-first century under a low–moderate emissions scenario. *J. Clim.* **28**, 4490–4512 (2015).
4. Perkins-Kirkpatrick, S. E. & Gibson, P. B. Changes in regional heatwave characteristics as a function of increasing global temperature. *Sci. Rep.* **7**, 12256 (2017).
5. Bates, L. M. & Hall, A. E. Stomatal closure with soil-water depletion not associated with changes in bulk leaf water status. *Oecologia* **50**, 62–65 (1981).
6. Roessler, P. G. & Monson, R. K. Midday depression in net photosynthesis and stomatal conductance in Yucca-Glauca—relative contributions of leaf temperature and leaf-to-air water-vapor concentration difference. *Oecologia* **67**, 380–387 (1985).
7. Tenhunen J. D., Pearcy R. W. & Lange O. L. in *Stomatal Function* (eds Zeiger, E. et al.) Ch. 15 (Stanford Univ. Press, 1987).
8. Tucci, M. L. S., Erismann, N. M., Machado, E. C. & Ribeiro, R. V. Diurnal and seasonal variation in photosynthesis of peach palms grown under subtropical conditions. *Photosynthetica* **48**, 421–429 (2010).
9. Kosugi, Y. & Matsuo, N. Seasonal fluctuations and temperature dependence of leaf gas exchange parameters of co-occurring evergreen and deciduous trees in a temperate broad-leaved forest. *Tree Physiol.* **26**, 1173–1184 (2006).
10. Koch, G. W., Amthor, J. S. & Goulden, M. L. Diurnal patterns of leaf photosynthesis, conductance and water potential at the top of a lowland rain-forest canopy in Cameroon—measurements from the Radeau-Des-Cimes. *Tree Physiol.* **14**, 347–360 (1994).
11. Olioso, A., Carlson, T. N. & Brisson, N. Simulation of diurnal transpiration and photosynthesis of a water stressed soybean crop. *Agric. For. Meteorol.* **81**, 41–59 (1996).
12. Cowan, I. R. & Farquhar, G. D. Stomatal function in relation to leaf metabolism and environment: stomatal function in the regulation of gas exchange. *Symposia Soc. Exp. Biol.* **31**, 471–505 (1977).
13. Bollig, C. & Feller, U. Impacts of drought stress on water relations and carbon assimilation in grassland species at different altitudes. *Agric. Ecosyst. Environ.* **188**, 212–220 (2014).
14. Koyama, K. & Takemoto, S. Morning reduction of photosynthetic capacity before midday depression. *Sci. Rep.* **4**, 4389 (2014).
15. Nelson, J. A., Carvalhais, N., Migliavacca, M., Reichstein, M. & Jung, M. Water-stress-induced breakdown of carbon–water relations: indicators from diurnal FLUXNET patterns. *Biogeosciences* **15**, 2433–2447 (2018).
16. Xu, H., Xiao, J. F. & Zhang, Z. Q. Heatwave effects on gross primary production of northern mid-latitude ecosystems. *Environ. Res. Lett.* **15**, 074027 (2020).
17. Baldocchi, D. et al. FLUXNET: a new tool to study the temporal and spatial variability of ecosystem-scale carbon dioxide, water vapor, and energy flux densities. *Bull. Am. Meteorol. Soc.* **82**, 2415–2434 (2001).
18. Running, S. W. et al. A continuous satellite-derived measure of global terrestrial primary production. *Bioscience* **54**, 547–560 (2004).
19. Xiao, J. F. et al. A continuous measure of gross primary production for the conterminous United States derived from MODIS and AmeriFlux data. *Remote Sens. Environ.* **114**, 576–591 (2010).
20. Anderson, M. C., Allen, R. G., Morse, A. & Kustas, W. P. Use of Landsat thermal imagery in monitoring evapotranspiration and managing water resources. *Remote Sens. Environ.* **122**, 50–65 (2012).
21. Sun, Y. et al. OCO-2 advances photosynthesis observation from space via solar-induced chlorophyll fluorescence. *Science* **358**, eaam5747 (2017).
22. Mu, Q., Heinsch, F. A., Zhao, M. & Running, S. W. Development of a global evapotranspiration algorithm based on MODIS and global meteorology data. *Remote Sens. Environ.* **111**, 519–536 (2007).
23. Fisher, J. B. et al. ECOSTRESS: NASA's next generation mission to measure evapotranspiration from the International Space Station. *Water Resour. Res.* **56**, 1–20 (2020).
24. Hook, S. J. et al. In-flight validation of ECOSTRESS, Landsat 7 and 8 thermal infrared spectral channels using the Lake Tahoe CA/NV and Salton Sea CA automated validation sites. *IEEE Trans. Geosci. Remote Sens.* **58**, 1294–1302 (2019).
25. Hulley, G., Shivers, S., Wetherley, E. & Cudd, R. New ECOSTRESS and MODIS land surface temperature data reveal fine-scale heat vulnerability in cities: a case study for Los Angeles County, California. *Remote Sens.* **11**, 2136 (2019).
26. Anderson, M. C. et al. Interoperability of ECOSTRESS and Landsat for mapping evapotranspiration time series at sub-field scales. *Remote Sens. Environ.* **252**, 112189 (2021).
27. Anderson, M. C. et al. An intercomparison of drought indicators based on thermal remote sensing and NLDAS-2 simulations with US drought monitor classifications. *J. Hydrometeorol.* **14**, 1035–1056 (2013).
28. Li, X., Xiao, J., Fisher, J. B. & Baldocchi, D. D. ECOSTRESS estimates gross primary production with fine spatial resolution for different times of day from the International Space Station. *Remote Sens. Environ.* **258**, 112360 (2021).
29. Hulley, G. C. et al. Validation and quality assessment of the ECOSTRESS level-2 land surface temperature and emissivity product. *IEEE Trans. Geosci. Remote Sens.* https://doi.org/10.1109/TGRS.2021.3079879 (2021).
30. Aragon, B., Houborg, R., Tu, K., Fisher, J. B. & McCabe, M. CubeSats enable high spatiotemporal retrievals of crop-water use for precision agriculture. *Remote Sens.* **10**, 1867 (2018).
31. Fisher, J. B. et al. The future of evapotranspiration: global requirements for ecosystem functioning, carbon and climate feedbacks, agricultural management, and water resources. *Water Resour. Res.* **53**, 2618–2626 (2017).
32. Turner, N. C., Schulze, E.-D. & Gollan, T. The responses of stomata and leaf gas exchange to vapour pressure deficits and soil water content. *Oecologia* **65**, 348–355 (1985).
33. Moore, G. W. & Heilman, J. L. Proposed principles governing how vegetation changes affect transpiration. *Ecohydrology* **4**, 351–358 (2011).
34. Hulley, G. C. & Hook, S. J. Generating consistent land surface temperature and emissivity products between ASTER and MODIS data for earth science research. *IEEE Trans. Geosci. Remote Sens.* **49**, 1304–1315 (2011).
35. Fisher, J. B., Whittaker, R. H. & Malhi, Y. ET Come Home: a critical evaluation of the use of evapotranspiration in geographical ecology. *Glob. Ecol. Biogeogr.* **20**, 1–18 (2011).
36. Talsma, C. J. et al. Partitioning of evapotranspiration in remote sensing-based models. *Agric. For. Meteorol.* **260**, 131–143 (2018).
37. Otkin, J. A. et al. Examining rapid onset drought development using the thermal infrared-based evaporative stress index. *J. Hydrometeorol.* **14**, 1057–1074 (2013).
38. Stavros, E. N. et al. ISS observations offer insights into plant function. *Nat. Ecol. Evolution* **1**, 0194 (2017).
39. Taylor, T. E. et al. OCO-3 early mission operations and initial (vEarly) XCO2 and SIF retrievals. *Remote Sens. Environ.* **251**, 112032 (2020).
40. Frankenberg, C. et al. The Orbiting Carbon Observatory (OCO-2): spectrometer performance evaluation using pre-launch direct sun measurements. *Atmos. Meas. Tech.* **8**, 301–313 (2015).
41. Bilger, W., Schreiber, U. & Bock, M. Determination of the quantum efficiency of photosystem-II and of nonphotochemical quenching of chlorophyll fluorescence in the field. *Oecologia* **102**, 425–432 (1995).
42. Maguire, A. J. et al. On the functional relationship between fluorescence and photochemical yields in complex evergreen needleleaf canopies. *Geophys. Res. Lett.* **47**, e2020GL087858 (2020).
43. Marrs, J. K. et al. Solar-induced fluorescence does not track photosynthetic carbon assimilation following induced stomatal closure. *Geophys. Res. Lett.* **47**, e2020GL087956 (2020).
44. Li, X. et al. Solar-induced chlorophyll fluorescence is strongly correlated with terrestrial photosynthesis for a wide variety of biomes: first global analysis based on OCO-2 and flux tower observations. *Glob. Change Biol.* **24**, 3990–4008 (2018).
45. Frankenberg, C. et al. New global observations of the terrestrial carbon cycle from GOSAT: patterns of plant fluorescence with gross primary productivity. *Geophys. Res. Lett.* **38**, L17706 (2011).

46. Li, X. & Xiao, J. F. Mapping photosynthesis solely from solar-induced chlorophyll fluorescence: a global, fine-resolution dataset of gross primary production derived from OCO-2. *Remote Sens.* **11**, 2563 (2019).
47. Liu, J. J. et al. Contrasting carbon cycle responses of the tropical continents to the 2015–2016 El Nino. *Science* **358**, eaam5690 (2017).
48. Parazoo, N. C. et al. Towards a harmonized long-term spaceborne record of far-red solar-induced fluorescence. *J. Geophys. Res.* **124**, 2518–2539 (2019).
49. He, L. Y. et al. Tracking seasonal and interannual variability in photosynthetic downregulation in response to water stress at a temperate deciduous forest. *J. Geophys. Res.* **125**, e2018JG005002 (2020).
50. Lin, C. J. et al. Evaluation and mechanism exploration of the diurnal hysteresis of ecosystem fluxes. *Agric. For. Meteorol.* **278**, 107642 (2019).
51. Magney, T. S. et al. Mechanistic evidence for tracking the seasonality of photosynthesis with solar-induced fluorescence. *Proc. Natl Acad. Sci. USA* **116**, 11640–11645 (2019).
52. Yang, X. et al. FluoSpec 2—an automated field spectroscopy system to monitor canopy solar-induced fluorescence. *Sensors (Basel)* **18**, 2063 (2018).
53. Miura, T., Nagai, S., Takeuchi, M., Ichii, K. & Yoshioka, H. Improved characterisation of vegetation and land surface seasonal dynamics in central Japan with Himawari-8 hypertemporal data. *Sci. Rep.* **9**, 15692 (2019).
54. Bessho, K. et al. An introduction to Himawari-8/9—Japan's new-generation geostationary meteorological satellites. *J. Meteorological Soc. Jpn* **94**, 151–183 (2016).
55. Schmit, T. J. et al. A closer look at the ABI on the GOES-R series. *Bull. Am. Meteorol. Soc.* **98**, 681–698 (2017).
56. Oh, S. M., Borde, R., Carranza, M. & Shin, I. C. Development and intercomparison study of an atmospheric motion vector retrieval algorithm for GEO-KOMPSAT-2A. *Remote Sens.* **11**, 2054 (2019).
57. Yang, J., Zhang, Z. Q., Wei, C. Y., Lu, F. & Guo, Q. Introducing the new generation of Chinese geostationary weather satellites, Fengyun-4. *Bull. Am. Meteorol. Soc.* **98**, 1637–1658 (2017).
58. Ouaknine, J. et al. The FCI on Board MTG: optical design and performances. In *International Conference on Space Optics—ICSO 2014* (eds Sodnik, Z. et al.) 1056323 (SPIE, 2014).
59. Wang, W. et al. An introduction to the Geostationary-NASA Earth Exchange (GeoNEX) products: 1. Top-of-atmosphere reflectance and brightness temperature. *Remote Sens.* **12**, 1267 (2020).
60. Yamamoto, Y., Ishikawa, H., Oku, Y. & Hu, Z. Y. An algorithm for land surface temperature retrieval using three thermal infrared bands of Himawari-8. *J. Meteorological Soc. Jpn.* **96B**, 59–76 (2018).
61. Yu, Y. & Yu, P. in *The GOES-R Series. A New Generation of Geostationary Environmental Satellites* (eds Goodman, S. J. et al.) Ch. 12 (2020).
62. Takenaka, H. et al. Estimation of solar radiation using a neural network based on radiative transfer. *J. Geophys. Res.* **116**, D08215 (2011).
63. Hashimoto, H. et al. Hourly GPP estimation in Australia using Himawari-8 AHI products. In *IGARSS 2020—2020 IEEE International Geoscience and Remote Sensing Symposium* 4513–4515 (IEEE, 2020).
64. Yan, K. et al. Evaluation of MODIS LAI/FPAR product collection 6. Part 1: consistency and improvements. *Remote Sens.* **8**, 359 (2016).
65. Moore, B. et al. The potential of the Geostationary Carbon Cycle Observatory (GeoCarb) to provide multi-scale constraints on the carbon cycle in the Americas. *Front. Environ. Sci.* https://doi.org/10.3389/fenvs.2018.00109 (2018).
66. Zoogman, P. et al. Tropospheric emissions: monitoring of pollution (TEMPO). *J. Quant. Spectrosc. Radiat. Transf.* **186**, 17–39 (2017).
67. Courrèges-Lacoste, G. B. et al. Knowing what we Breathe: Sentinel 4: a Geostationary Imaging UVN Spectrometer for Air Quality Monitoring. In *International Conference on Space Optics—ICSO 2016* (eds Karafolas, N. et al.) 105621J (SPIE, 2017).
68. Wekerle, T., Pessoa, J. B., da Costa, L. & Trabasso, L. G. Status and trends of smallsats and their launch vehicles—an up-to-date review. *J. Aerosp. Technol. Manag.* **9**, 269–286 (2017).
69. Ryswyk, M. V. Planet announces 50 cm SkySat imagery, tasking dashboard and up to 12× revisit. *Planet* (9 June 2020); https://www.planet.com/pulse/tasking-dashboard-50cm-12x-revisit-announcement/
70. Blackwell, W. J. et al. An overview of the TROPICS NASA Earth Venture mission. *Q. J. R. Meteorol. Soc.* **144**, 16–26 (2018).
71. Gao, F., Masek, J., Schwaller, M. & Hall, F. On the blending of the Landsat and MODIS surface reflectance: predicting daily Landsat surface reflectance. *IEEE Trans. Geosci. Remote Sens.* **44**, 2207–2218 (2006).
72. Franco, A. C. & Luttge, U. Midday depression in savanna trees: coordinated adjustments in photochemical efficiency, photorespiration, CO_2 assimilation and water use efficiency. *Oecologia* **131**, 356–365 (2002).
73. Keller, M., Schimel, D. S., Hargrove, W. W. & Hoffman, F. M. A continental strategy for the National Ecological Observatory Network. *Front. Ecol. Environ.* **6**, 282–284 (2008).

Acknowledgements

This study was supported by the NASA's ECOSTRESS Science and Applications Team (80NSSC20K0167) (J.X.), NASA's Climate Indicators and Data Products for Future National Climate Assessments (NNX16AG61G) (J.X.), the National Science Foundation (Macrosystem Biology & NEON-Enabled Science program: DEB-2017870, EF-1638688) (J.X.), NASA's ECOSTRESS (J.B.F.), NASA Earth Exchange (NEX) from NASA's Earth Science Division (H.H.), the Virtual Laboratory (VL) project by the Ministry of Education, Culture, Sports, Science and Technology (MEXT), Japan (K.I.), a research grant of the Japan Society for the Promotion of Science (JSPS), KAKENHI (20K20487) (K.I.), and the Earth Science Division OCOST program (N.C.P.). J.B.F. and N.C.P. carried out their research at the Jet Propulsion Laboratory, California Institute of Technology, under a contract with NASA. California Institute of Technology. Government sponsorship acknowledged. A portion of these data were produced by the OCO-3 project at the Jet Propulsion Laboratory, California Institute of Technology, and obtained from the OCO-3 data archive at the NASA Goddard Earth Science Data and Information Services Center. G. Halverson provided ECOSTRESS visualization. Himawari-8 AHI-based LST data used in this study were provided by Y. Yamamoto, Chiba University, Japan.

Author contributions

J.X. conceived the idea. J.X., J.B.F., H.H., K.I. and N.C.P. designed the research, conducted the analyses, interpreted the data and wrote the paper.

Competing interests

The authors declare no competing interests.

Additional information

Supplementary information The online version contains supplementary material available at https://doi.org/10.1038/s41477-021-00952-8.

Correspondence should be addressed to J.X.

Peer review information *Nature Plants* thanks Gerbrand Koren, Steve Running and Changliang Shao for their contribution to the peer review of this work.

Reprints and permissions information is available at www.nature.com/reprints.

Publisher's note Springer Nature remains neutral with regard to jurisdictional claims in published maps and institutional affiliations.

nature research

Corresponding author(s): Jingfeng Xiao

Last updated by author(s): 02-13-2021

Reporting Summary

Nature Research wishes to improve the reproducibility of the work that we publish. This form provides structure for consistency and transparency in reporting. For further information on Nature Research policies, see our Editorial Policies and the Editorial Policy Checklist.

Statistics

For all statistical analyses, confirm that the following items are present in the figure legend, table legend, main text, or Methods section.

n/a	Confirmed	
☐	☒	The exact sample size (*n*) for each experimental group/condition, given as a discrete number and unit of measurement
☒	☐	A statement on whether measurements were taken from distinct samples or whether the same sample was measured repeatedly
☒	☐	The statistical test(s) used AND whether they are one- or two-sided *Only common tests should be described solely by name; describe more complex techniques in the Methods section.*
☒	☐	A description of all covariates tested
☒	☐	A description of any assumptions or corrections, such as tests of normality and adjustment for multiple comparisons
☒	☐	A full description of the statistical parameters including central tendency (e.g. means) or other basic estimates (e.g. regression coefficient) AND variation (e.g. standard deviation) or associated estimates of uncertainty (e.g. confidence intervals)
☒	☐	For null hypothesis testing, the test statistic (e.g. *F*, *t*, *r*) with confidence intervals, effect sizes, degrees of freedom and *P* value noted *Give P values as exact values whenever suitable.*
☒	☐	For Bayesian analysis, information on the choice of priors and Markov chain Monte Carlo settings
☒	☐	For hierarchical and complex designs, identification of the appropriate level for tests and full reporting of outcomes
☒	☐	Estimates of effect sizes (e.g. Cohen's *d*, Pearson's *r*), indicating how they were calculated

Our web collection on statistics for biologists contains articles on many of the points above.

Software and code

Policy information about availability of computer code

Data collection	No software was used in data collection.
Data analysis	Softwares sued for data analysis include g++, ArcMap 10, Matlab, and Python.

For manuscripts utilizing custom algorithms or software that are central to the research but not yet described in published literature, software must be made available to editors and reviewers. We strongly encourage code deposition in a community repository (e.g. GitHub). See the Nature Research guidelines for submitting code & software for further information.

Data

Policy information about availability of data

All manuscripts must include a data availability statement. This statement should provide the following information, where applicable:

- Accession codes, unique identifiers, or web links for publicly available datasets
- A list of figures that have associated raw data
- A description of any restrictions on data availability

The data availability statement is included at the end of the manuscript.

Field-specific reporting

Please select the one below that is the best fit for your research. If you are not sure, read the appropriate sections before making your selection.

☐ Life sciences ☐ Behavioural & social sciences ☒ Ecological, evolutionary & environmental sciences

For a reference copy of the document with all sections, see nature.com/documents/nr-reporting-summary-flat.pdf

Ecological, evolutionary & environmental sciences study design

All studies must disclose on these points even when the disclosure is negative.

Study description	This is a perspective article on the emerging satellite observations for studying diurnal cycling of ecosystem processes. We did not directly carry out any measurements.
Research sample	We did not directly carry out any measurements.
Sampling strategy	We did not directly carry out any measurements.
Data collection	We used satellite data that are publicly available.
Timing and spatial scale	The data that we used span the period from 2018 to 2020.
Data exclusions	We did not directly carry out any measurements.
Reproducibility	Our visual results are based on publicly available datasets and can be fully reproduced.
Randomization	We did not directly carry out any measurements.
Blinding	We did not directly carry out any measurements.

Did the study involve field work? ☐ Yes ☒ No

Reporting for specific materials, systems and methods

We require information from authors about some types of materials, experimental systems and methods used in many studies. Here, indicate whether each material, system or method listed is relevant to your study. If you are not sure if a list item applies to your research, read the appropriate section before selecting a response.

Materials & experimental systems

n/a	Involved in the study
☒	☐ Antibodies
☒	☐ Eukaryotic cell lines
☒	☐ Palaeontology and archaeology
☒	☐ Animals and other organisms
☒	☐ Human research participants
☒	☐ Clinical data
☒	☐ Dual use research of concern

Methods

n/a	Involved in the study
☒	☐ ChIP-seq
☒	☐ Flow cytometry
☒	☐ MRI-based neuroimaging